See discussions, stats, and author profiles for this publication at: https://www.researchgate.net/publication/231641985

Biocatalytic Generation of Ppy-Enzyme-CNT Nanocomposite: From Network Assembly to Film Growth

ARTICLE in THE JOURNAL OF PHYSICAL CHEMISTRY C · JANUARY 2007

Impact Factor: 4.77 · DOI: 10.1021/jp0671594

CITATIONS READS
48 61

9 AUTHORS, INCLUDING:



Chang Li

Xin Xiang Medical University

391 PUBLICATIONS 13,097 CITATIONS

SEE PROFILE



Peter Vee Sin Lee

University of Melbourne

100 PUBLICATIONS 1,004 CITATIONS

SEE PROFILE



Haifeng Bao

Wuhan Textile University

27 PUBLICATIONS **972** CITATIONS

SEE PROFILE



Shabbir M Moochhala

Centre for Molecular Diagnostics Temasek Po...

218 PUBLICATIONS 6,664 CITATIONS

SEE PROFILE

Biocatalytic Generation of Ppy-Enzyme-CNT Nanocomposite: From Network Assembly to Film Growth

Xiaoqiang Cui,^{†,‡} Chang Ming Li,*,^{†,‡} Jianfeng Zang,^{†,‡} Qin Zhou,^{†,‡} Ye Gan,^{†,‡} Haifeng Bao,^{†,‡} Jun Guo,[§] Vee. S. Lee,^{||} and Shabbir M. Moochhala^{||}

School of Chemical and Biomedical Engineering, Nanyang Technological University, 70 Nanyang Drive, Singapore 637457, Center for Advanced Bionanosystems, Nanyang Technological University, 70 Nanyang Drive, Singapore 637457, School of Materials Science and Engineering, Nanyang Technological University, Nanyang Drive, Singapore 639798, and Defence Medical & Environmental Research Institute, DSO National Laboratories, Singapore 117510

Received: October 31, 2006; In Final Form: December 2, 2006

Nanocomposites have attracted great research and development interests. Lactate oxidase (LOD) in the presence of lactate was used to initiate the polymerization of pyrrole monomer with and without carbon nanotube (CNT) presence to produce a 2- or 3-component nanocomposite. We found that the formation mechanisms for the 2- and 3-component nanocomposites were different—from network assembly to film growth. Enzyme molecules served as the seeds for polymerization without CNT presence and preferentially resulted in the formation of nanoparticles. In this case, an interesting self-assembly of the nanoparticles was observed. However, when CNTs were introduced into the reaction system, they functioned as the seeds for the polymerization and a CNT-networked nanocomposite film was formed. The morphology, components, and the thickness of the composite film could be easily tailored by the reaction time, the ratio of pyrrole to CNTs, and the amount of enzyme. The application of the nanocomposite for the lactase biosensor and the effects of components of the nanocomposite on both sensing and electronic properties were also studied, demonstrating their novelty and superior properties. This work is the first one to report the biocatalytic production of polypyrrole (Ppy)-enzyme-CNT, a 3-component nanocomposite, its formation mechanism, and its applications.

Introduction

Over the last two decades, conducting polymers have attracted great research interest due to their superior chemical/physical properties and important applications. They have been proven to be a very suitable matrix to trap enzyme for biosensors with fast response time, high sensitivity, and great versatility in analytical tools. Among them, Ppy has been extensively investigated in biosensors and drug delivery systems because of their excellent stability and biocapability. Ppy has been used in biosensors with different immobilized biomolecules in its films on different substrates. The order to improve the performance of biosensors or other devices, different approaches to functionalize Ppy have been developed. For example, Ppy derivatives have been investigated to improve immobilization of protein, Sa,9 DNA, 10,11 or the use of copolymerization to get improved permeability or biodegradable composites.

Since the first discovery in 1991,¹⁴ CNTs have been studied extensively because of their high surface area, excellent electrical conductivity, and unique nanostructures.^{15,16} Since Ppy could provide an ideal matrix to home CNTs, different CNT-Ppy

hybrid nanocomposites have been recently developed for energy storage systems, nanoelectronics, and bio/chemical sensors. ^{17–21}

Two approaches have been reported to produce Ppy and Ppy nanocomposites. Electrochemical polymerization is the most widely used method due to its advantage of easy immobilization of biomolecules into the Ppy matrix during polymerization. Entrapment or covalent immobilization of biomolecules into Ppy²² or Ppy-CNTs matrix^{17,23} is used. However, the electrochemical method is limited to substrates related to electrodes and low throughput production.²⁴ Ppy can be also chemically synthesized, a process which is based on the oxidation of pyrrole monomer by oxidants such as ferric chloride.²⁵ The method is apparently not suitable for biomolecule immobilization during preparation owing to the possibility of the denaturing of biomolecules by the oxidative chemicals. Recently, enzymes have been employed as a biocatalyst to synthesize metal nanoparticles^{26–28} and/or nanopatterned materials.²⁹ The main advantage of the method offers a new strategy to particularly prepare a biomolecules-incorporated nanocomposite. Most recently, Ramanavicius and co-workers prepared Ppy nanoparticles by glucose oxidase-initiated polymerization.³⁰ Nanotechnology is rapidly evolving to engineering new materials. It is very attractive to create a novel approach that can entrap both nanostructured materials such as CNTs and biomolecules such as proteins into the Ppy matrix for superior nanocomposites in different important applications.

In this work, we used an enzymatically catalytic polymerization method to prepare Ppy-LOD-CNT or Ppy-LOD, a 2- or 3-component hybrid nanocomposite. Enzyme LOD was used to initiate the polymerization of pyrrole in the presence of

^{*} Corresponding author. Tel: +65 67904485. Fax: +65 67911761. E-mail: ecmli@ntu.edu.sg (C.M. Li).

 $^{^\}dagger$ School of Chemical and Biomedical Engineering, Nanyang Technological University.

[‡] Center for Advanced Bionanosystems, Nanyang Technological University.

 $[\]S$ School of Materials Science and Engineering, Nanyang Technological University.

^{||} Defence Medical & Environmental Research Institute, DSO National Laboratories.

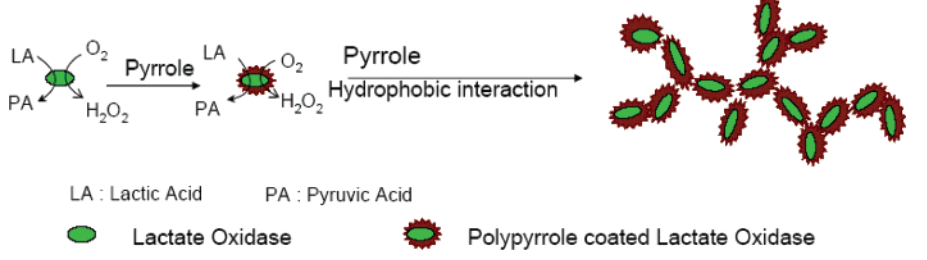


Figure 1. Schematic of the process of Ppy-LOD self-assembly and composite formation by an enzymatic catalysis reaction.

lactate. The preparation, formation mechanism, and properties of the 2- and 3-component hybrid nanocomposites were studied by AFM, field-emission SEM (FE-SEM), and TEM. The mechanisms of formation of the nanocomposite were investigated with and without CNTs. Detailed nanostructure features of the nanocomposites were revealed. The nanocomposites were successfully applied for electrochemical lactate biosensors. The effects of the nanocomposite components on the sensing and the electronic properties were also investigated. To our knowledge, such an extensive study on the biocatalysis-formed Ppy-LOD-CNT nanocomposite has never before been reported.

Experimental Methods

Lactate oxidase (EC 232-841-6 from *Pediococcus* species) lyophilized powder containing 41 units/mg solid and pyrrole were obtained from Sigma and were used as received. Lactate and other chemicals were all of analytical grade. Water was purified with a Millipore Milli-Q-System. Multiwall carbon nanotubes (MCNTs) were purchased from Shenzhen Nanotech Co. Ltd.

UV—vis absorption spectra were recorded by the Hitachi U-2800 UV—vis spectrophotometer (Japan). AFM images were captured with tapping mode at ambient temperature by an atomic force microscope (AFM) (SPM 3000, Veeco Instruments Inc., USA). FE-SEM was performed on the JEOL (JSM-6700F) at an acceleration voltage of 5 kV and a working distance of 8 mm. Transmission electron microscopy (TEM) images were obtained on JEM 2100 (JEOL, Japan) with the working voltage at 200 kV.

A freshly cleaved mica surface was used for adsorption of Ppy nanoparticles and AFM measurements. To prepare the sample, 2 μ L of the mixture of polymerization solution were equally distributed on a 3-mm-diameter mica surface and dried at 50 °C in the oven. The surfaces were then thoroughly rinsed with distilled water to remove the excess of pyrrole monomer, lactate, pyruvic acid, and salts. The samples were dried at room temperature in air for 24 h.

For preparation of a Ppy-CNT nanocomposite, MCNTs were refluxed in 3 M HNO₃ for 3 days. After precipitation and centrifugation, the suspension was washed three times at least by water until neutral pH achieved. Finally, the solid sample was dried in a vacuum for about 4 h. MCNTs were then dissolved to have a concentration of 3.0 mg/mL in water for use.

The nanocomposite was prepared by the following procedure. A mixture of 100 μ L of pyrrole (200 mM), 10 μ L of LOD (10 mg/mL), and 10 μ L of lactate (0.2 M) in four 1.5-mL centrifuge vials was made first. A CNT solution (0.3 mg/mL) was prepared and ultrasonicated for 1 min before every use. Then different volumes of CNTs (0, 2, 10, 50 μ L) were added into the four vials containing the pyrrole-LOD-lactate mixture, respectively. All solutions were prepared in 20 mM PBS buffer (pH 7.0). After 1-min-ultrasonic mixing, all prepared solutions were put in a dark container and kept at room temperature. Another

approach to preparing the solutions was to keep the CNTs constant, for example, 50 μ L, and then to add different volumes of the pyrrole-LOD-lactate mixture for adjustment of the ratio of different components. The vials were re-ultrasonicated for 1 min before the UV-vis measurement or preparation for SEM and TEM measurements. For TEM measurement, the vials were centrifuged for about 10 min at 12000 rpm and washed with the distilled water 3 times. Then 5 μ L of resuspended CNT nanocomposite in water was dropped on copper grids and dried overnight at room temperature. For SEM, the mixture was dropped directly on copper grids or a gold film formed on a glass slide.

Cyclic voltammetric (CV) and chronoamperometry measurements were performed with a CHI-660B electrochemical station (Ch Instruments Inc., Texas). A three-electrode system comprised of the nanocomposite-modified Pt electrode (2.0-mm diameter) as working electrode, a platinum wire as auxiliary electrode, and a Ag/AgCl as the reference electrode was employed for all electrochemical experiments. CV measurements were carried out in a static electrochemical cell at 25 °C, while amperometric experiments were carried out in a stirred cell with successive additions of lactate standard solution to 20 mL of PBS. For preparation of a LOD/Ppy-modified electrode, 2 µL of 1 mg/mL enzyme mixture were deposited on a Pt electrode surface and dried at room temperature. The drop-anddry procedure was repeated five times to make 10 µL of polymerization solution deposited on the electrode surface. The electrode was thoroughly washed with PBS buffer and then used for electrochemical measurements.

Current—voltage measurements were performed on a Cascade MicroTech probe station, model: SUMMIT 11971B and Agilent Semiconductor Parameter Analyzer model E5270B. For I–V measurements, 2 μ L of the Ppy/LOD or Ppy/CNT/LOD nanocomposite suspension was placed between two homemade gold electrodes with a 2-mm gap and dried under vacuum.

Results and Discussion

It is known that lactate oxidase (LOD) catalyzes the conversion of lactate to pyruvic acid and hydrogen peroxide in the presence of oxygen. In our work, LOD was used to catalyze the oxidation of lactate for producing hydrogen peroxide and thus initializing the polymerization of the pyrrole monomer by oxidation reaction (schematically illustrated as in Figure 1). The negatively charged LOD molecules (IP pH 4.6)31 served as the seeds to electrostatically attract the positively charged oligomers of Ppy in neutral buffer (pH 7.0 PBS buffer) for polymerization. Thus, LOD played a bifunctional role: catalyst and polymerization seed. The visible light spectrum was successfully used to reveal the changes in electron states of the conjugated double bond in electrochemically polymerized Ppy.³² In this work, UV-vis spectroscopy was employed to monitor the polymerization of the pyrrole monomer. As shown in Figure 2A, a strong and sharp absorption peak at 460 nm appeared during the

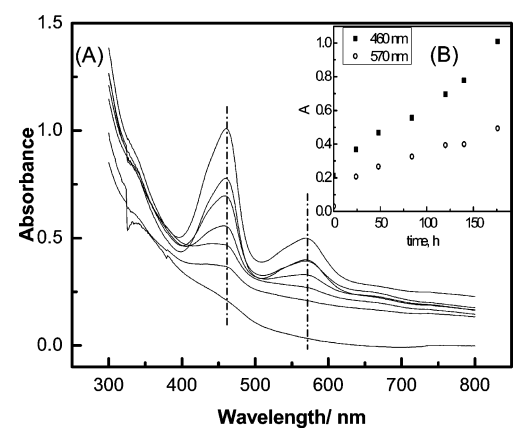


Figure 2. UV-vis characterization of the formation of Ppy-LOD nanoparticles in 0.02 M PBS, pH 7.0, containing 1 mg/mL LOD, 20 mM lactate, and 200 mM pyrrole. The reaction times were 0, 24, 48, 84, 120, 140, and 176 h (from bottom to top). Inset is the absorbance at 460 and 570 nm vs the reaction time.

enzymatic catalytic reaction. After a 4-day reaction, a new peak also appeared at 570 nm. The control experiments of the mixture of LOD + lactate or the mixture of pyrrole + LOD, or the mixture of pyrrole + lactate were carried out under the same conditions and did not show any peak over the 300-800-nm range after 5 days (data not shown). The absorption peak at 460 nm was attributed to electron transition from valence band to antibipolaron band in Ppy, $^{\rm 32}$ which was the characteristic Ppy absorption peak for the formation of Ppy oligomers.²⁵ The peak at 570 nm could be assigned to the polaron formation in the Ppy structure.³² Almost linear dependence of the adsorption intensity of Ppy vs reaction time was detected at both peaks at $\lambda = 460$ nm and $\lambda = 570$ nm (Figure 2B). The growing rate showed by the slope in Figure 2B for 570 nm was slightly lower than that for 460 nm. This might indicate that the polaron formation was a consequent step after the Ppy oligomers

formation. The intensities of peaks at 460, 570, and 800 nm were assigned to $\pi - \pi^*$ transition, polaron, and bipolaron, respectively.³² These peaks were often used to indicate the insulating neutral state, polaron state, and bipolaron state of structures of Ppy.33 In our experiments, no peak at 800 nm was observed in UV-vis spectroscopy, which might indicate that Ppy formed by enzymatic catalysis had a lower doping level. The spectrum was in agreement with the optical results obtained from reduced Ppy by electrochemical polymerization.^{33,34} The result possibly demonstrated that the enzymatic polymerization of Ppy employed by us could completely stabilize the polaron state, but not to couple with each other during the polymerization, thus making it difficult for the polymer segments to produce a bipolaron state from a polaron state.³⁴ As the reaction time was increased, the color of the solution turned to yellow and precipitation was observed after the reaction for 4 days. No shift of peak position at 460 nm was observed even after 7-day reaction. This possibly indicated that the Ppy was Ppy I in longer chains (number of pyrrole units >64, $\lambda = 450-470$ nm). 35 The electrostatic attraction between Ppy and LOD could cause the newly synthesized Ppy oligomers surrounding LOD molecules to form nanoparticles. When the nanoparticles were growing big enough, the LOD could be thoroughly covered and the hydrophobic interaction between Ppy would induce the assembly of nanoparticles to bigger aggregations, thus resulting in precipitation (Figure 1). In order to further prove the analysis above, AFM was used to investigate the assembly process of the nanoparticles.

The experimental results in Figure 2 indicate that lactate oxidase not only controls the concentration of hydrogen peroxide generated in the mixture, but also acts as seeds for polymerization. Therefore, the concentration of the LOD would definitely affect the growing speed and the concentration of the nanoparticles. As shown in Figure 3, parts A and B, in the reactant solution with a lower concentration of LOD as 1 mg/mL for 24-h reaction, the nanoparticles were quite uniform (20 \pm 10

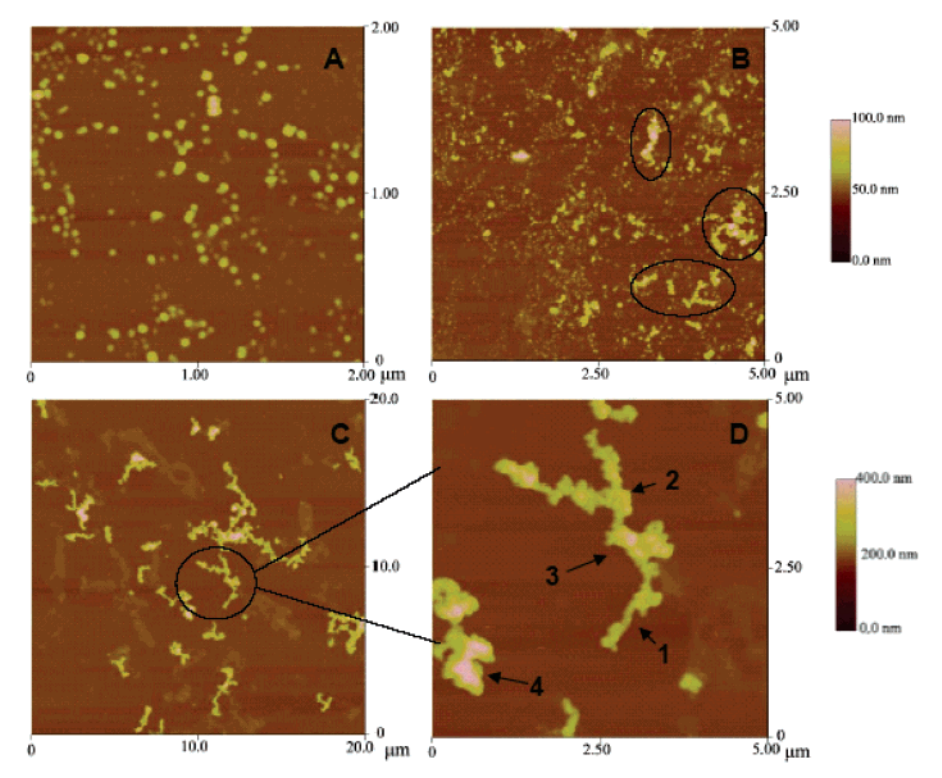
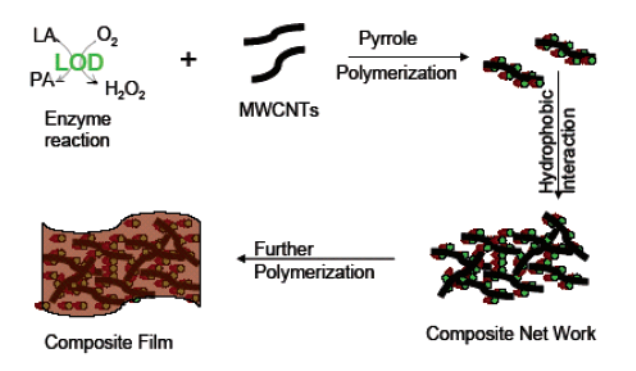


Figure 3. AFM images of Ppy-LOD nanoparticles on a mica surface with different reaction time 24 h (A,B), 72 h (C,D), and with different concentrations of LOD of 1.0 mg/mL (A,C,D) and 2.0 mg/mL (B). Experimental conditions are the same as those given in Figure 2.



LA: Lactic Acid PA: Pyruvic Acid Polypyrrole and LOD composite

Figure 4. Schematic representation of the formation of CNT-PpyLOD nanocomposite by enzymatic catalysis reaction.

nm in diameter, from section analysis) and monodispersed in the solution. When the enzyme concentration increased to 2 mg/ mL, the particle size appeared larger (25 \pm 10 nm in diameter) and the surface concentration of the nanoparticles was almost as double that generated from 1 mg/mL LOD. Most importantly, we observed that some of the nanoparticles aggregated to form a networked or necklace chainlike structure with the length of a few hundred nanometers (circle area in Figure 3B). This phenomenon could be attributed to the high concentration of nanoparticles in the solution produced by enzymatic reaction. In order to further investigate the effect of the reaction time on nanoparticle formation, we used the lower concentration of LOD (1.0 mg/mL) for sample preparation. As shown in Figure 3C, after 72-h reaction in a solution with 1.0 mg/mL LOD, most of the nanoparticles were aggregated to form a nanoscale networked or necklacelike structure with lengths of $1-5 \mu m$. More detailed information on the nanoparticles assembly of the circle could be obtained by zooming in on the AFM images area in Figure 3C, which clearly showed that the "necklace" assemblies consisted of very uniform nanoparticles attached to each other

in a line, fork, or network shape. The corresponding phase images were consistent with the morphology conclusions (data not shown). Even after thorough washing, some assembly features on a mica surface shown in Figure 3C could be still observed, indicating good stability of the nanoscale structure. From the AFM analysis on the sectioned sample, the nanoparticles were very uniform with the size of 65 \pm 4 nm in the necklace chain. The necklace chain showed different heights of 133, 199, and 258 nm clearly. These different heights could be assigned to the double, triple, and tetra particle assemblies, since the heights are exactly $2\times$, $3\times$, and $4\times$ the size of a single nanoparticle showed in Figure 3C. The single, double, triple, and tetra particle assembly are shown in Figure 3D, 1-4 respectively. This assembly could be fairly ascribed to the hydrophobic interaction between Ppy nanoparticles in the colloidal solution. In fact, precipitation could be visually observed when the reaction was conducted for more than 4 days. This was apparently caused by highly developed, assembled large particles from the growth, which could not suspend in the solution.

CNTs can provide an ideal matrix for depositing Ppy film because of its intrinsic properties of high surface area, high electrical conductivity, and unique hollow-size geometry. Recently, CNT and Ppy hybrid nanocomposites have been developed for super capacitor or chemical sensors using chemical or electrochemical methods. The Zhang and coworker have reported that a certain amount of CNTs could act as seeds for the chemical formation of polyaniline. Here, we tried to use the CNTs as seeds for polymerization of Ppy by enzymatic reaction. Thus, a novel nanocomposite containing LOD-Ppy or LOD-Ppy-CNT could be fabricated as shown in Figure 4.

The nanocomposite formation process after addition of CNTs in the enzymatic reaction system was investigated by SEM. The results in Figure 5 show that without addition of CNTs, Ppy nanoparticles with the size of about 100 nm were highly

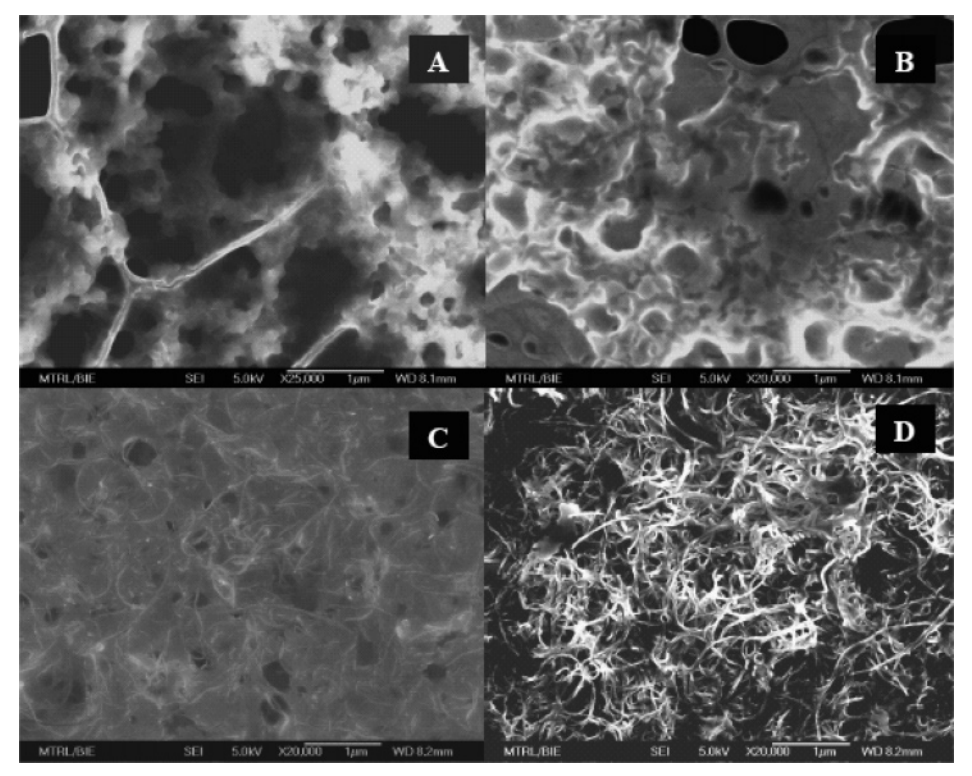


Figure 5. FE-SEM images of the nanocomposites after 48-h reaction with different volumes of MCNT (0.3 mg/mL): $0 \mu L$ (A), $2 \mu L$ (B), $10 \mu L$ (C), and $50 \mu L$ (D) in $100 \mu L$ of pyrrole-LOD mixture containing 1.0 mg/mL LOD, 200 mM pyrrole, 20 mM lactate in PBS (0.02 M, pH = 7.0).

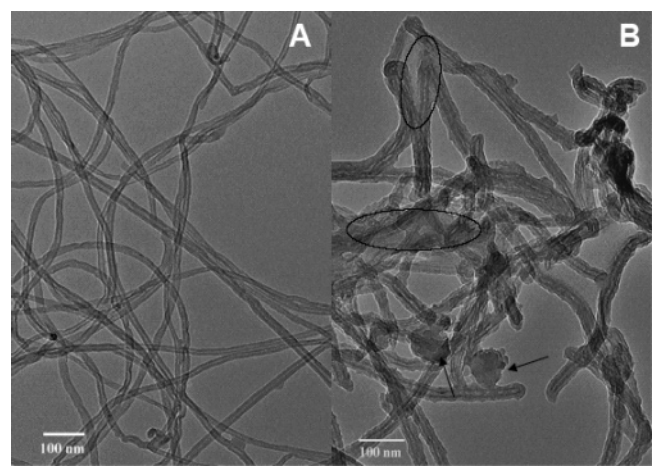


Figure 6. TEM images of pristine (A) and modified (B) multiwall carbon nanotubes; (B) was obtained under the same experimental conditions as shown in Figure 5D. The composite was washed 3 times with water before measurements.

aggregated and assembled into the network nanostructure. Since a washing step was not performed for the sample preparation before SEM measurements but it was done for the AFM sample, the surface concentration of the network-structured nanocomposite should be much higher than that shown in the AFM images. The result is in agreement with the AFM results in Figure 3 and further supports the scheme that we proposed in Figure 1. With addition of CNTs, the morphology of the nanocomposite changed greatly (Figure 5B-D). When we added a very small volume (2 μ L of 0.3 mg/mL) of CNTs in the system (100 μ L), the nanoparticles were seldom seen and the Ppy was surrounded by a very few CNT seeds, and thus formed island Ppy (Figure 5B). When more CNTs (10 μ L of 0.3 mg/mL) were added, no nanoparticle was observed any more and a uniform

Ppy film containing CNTs was observed in the product (Figure 5C). When 50 μ L (0.3 mg/mL) of CNTs were added in the reaction solution, a Ppy-coated CNT-network nanostructure was obtained and some areas were connected with Ppv thin film (Figure 5D). It might indicate that there was competition between enzyme molecules and CNTs as seeds for Ppy nucleation and polymerization. Thus, our experimental results demonstrated that even after introduction of CNTs into the reaction system, the Ppy-CNT-LOD nanocomposite could be a network structure formed by CNT-seeded polymerization or a film structure formed by enzyme catalytic polymerization. In the polymerization procedure, the LOD would definitely be entrapped into the nanocomposite.

The formation of a Ppy-coated CNT-network nanostructure was further confirmed by TEM images (Figure 6). Figure 6A shows the TEM image of multiwall carbon nanotubes (MCNTs) before modification with Ppy-LOD. It can be seen that the MCNTs are endless with a very smooth surface. Figure 6B shows a representative image of Ppy-LOD-modified CNTs. It is interesting to see that CNTs are almost uniformly covered by Ppy film with about 7-nm thickness. Some areas shown in the figure are connected together. This may be due to the hydrophobic interaction of Ppy and further developed to form a Ppy bulk film (indicated by circles in Figure 6D). It was also observed that few nanoparticles of Ppy were attached on MCNTs surface (indicated by arrows), which could further confirm the competition between two types of seeds.

To gain further insight into the nanocomposite formation, in which what factors can affect the morphology of the CNT-Ppy-LOD nanocomposite, more delicately designed control experiments were performed. According to the experiments discussed in Figure 5, the volume of CNTs was fixed at 50 μ L of 0.3 mg/mL and 10, 40, 150, and 400 μ L of pyrrole-LOD-lactate mixture were added into the reaction system, respectively (a

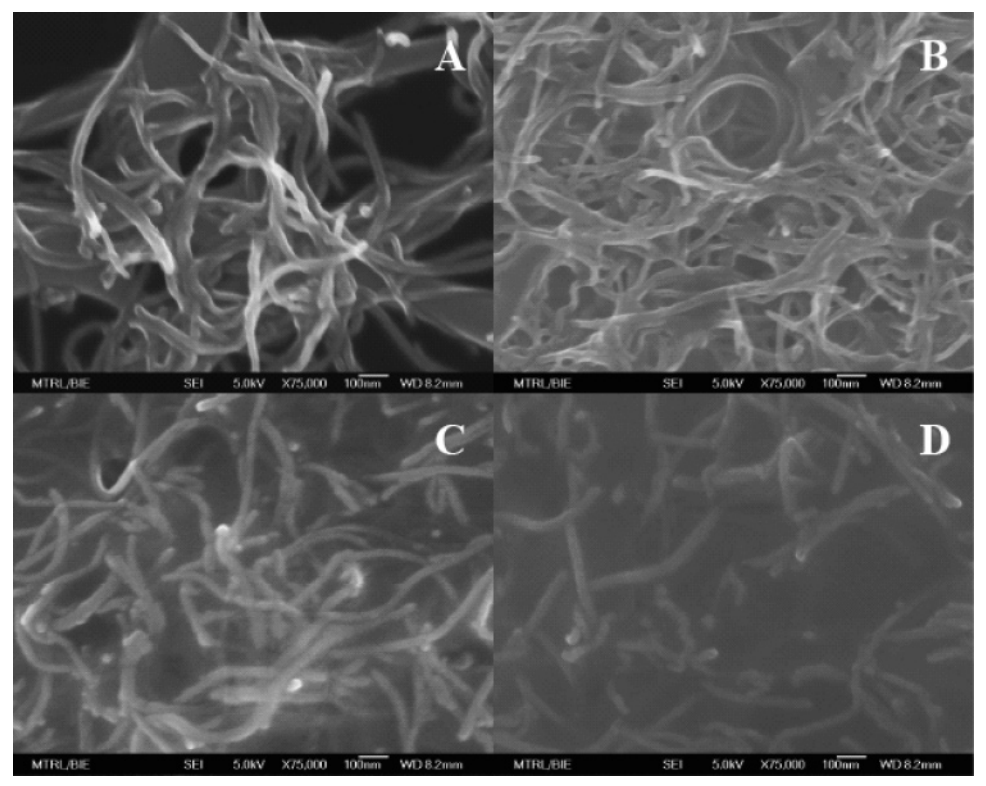


Figure 7. FE-SEM images of nanocomposite after 48-h reaction with different ratios of PPY-LOD to MCNT. The samples were prepared by keeping CNTs constant as 50 μL (0.3 mg/mL) while adding the pyrrole-LOD mixture containing 1.0 mg/mL LOD, 200 mM pyrrole, 20 mM lactate in PBS (0.02 M, pH = 7.0) with different volumes: 10 μ L (A), 40 μ L (B), 150 μ L (C), and 400 μ L (D).

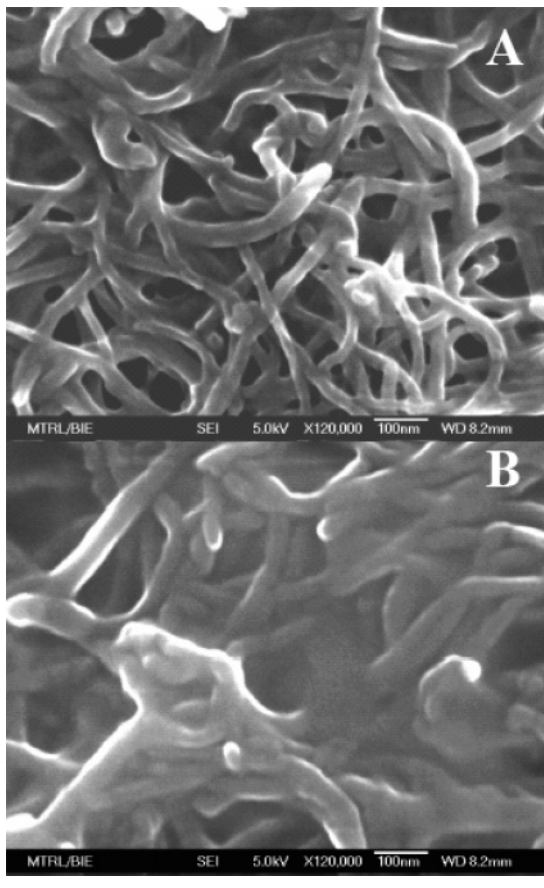


Figure 8. FE-SEM images of PPY-LOD-CNT composite after 1-day (A) and 4-day (B) reactions. Experimental conditions are given in Figure 5D.

detailed description is in the Experimental Methods section). Figure 7 shows the typical SEM images of the samples after 48-h reaction for the designed experiments. In a small amount of pyrrole-LOD-lactate mixture, the surface concentration of CNTs was high and the polymerization preferentially happened onto the CNT surface. The modified CNTs were attached to each other to form a network structure (Figure 7A,B). With the increase of the volume of pyrrole-LOD-lactate mixture, the CNTs were fully covered by Ppy and then formed bulk CNT-containing film (Figure 7C,D). The experimental results demonstrated that the nanocomposite structures could be controlled easily by adjusting the ratio of the concentration of CNT to that of the pyrrole-LOD-lactate mixture.

The effect of reaction time on the nanocomposite formation was also investigated by studies of the FE-SEM morphology of the nanocomposites. The sample was prepared with the same conditions as indicated in Figure 5D and was monitored each day. Figure 8, parts A and B, shows the SEM images after the reaction for 1 and 4 days, respectively. After the 4-day reaction, the CNT-Ppy-LOD composites were grown from 20-40 nm on the first day to 30-55 nm in diameter. The results showed that the Ppy-LOD was growing between the spaces of Ppycoated CNTs and made the bulk film of the nanocomposite. These results elucidated that the nanocomposite structure could be controlled not only by the ratio of concentrations of reactants but also by the reaction time. The controllable nanoscale structures, morphologies, and components of Ppy-LOD-CNTs nanocomposite could be tailored to different advanced electronic devices or biosensor devices for important applications. 17-21

The beauty of the biocatalytic method is its ability to onestep fabricate LOD-Ppy and LOD-Ppy-CNT nanocomposites

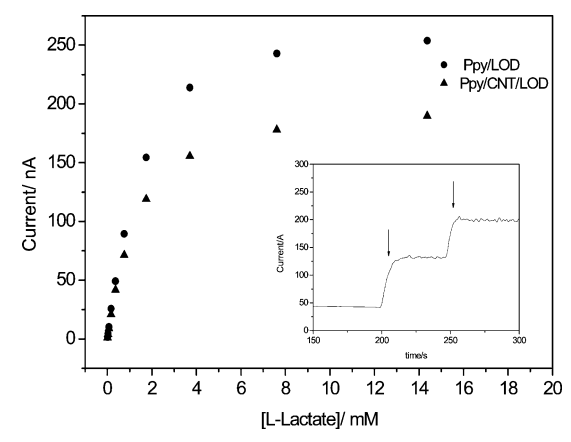


Figure 9. Calibration curve of nanocomposite-modified Pt electrodes. Inset is the chronoamperometric response of injection of 0.5 mM L-lactate for Ppy/LOD-modified electrode. E = +0.7 V; all experiments were taken in pH 7.0 PBS, 0.15 M NaCl.

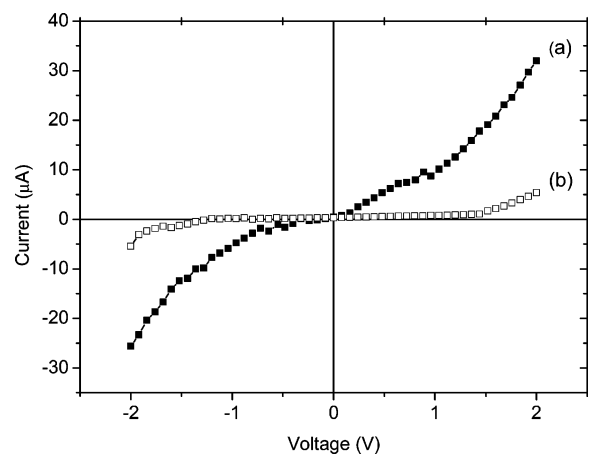


Figure 10. Current—voltage curves obtained from nanocomposite of Ppy-CNT-LOD (a) and Ppy-LOD (b).

for electrochemical enzyme sensors. The applications of the nanocomposites for lactate biosensor were investigated. The nanocomposite was formed on a Pt electrode for electrochemically detecting H2O2 generated from lactate under LOD catalysis. As shown in Figure 9, the response was very fast and sensitive to the detection of lactate in solution. The detection limit obtained was 10 µM for both Ppy-LOD and Ppy-CNT-LOD systems. Surprisingly, the maximum reaction rates calculated from Figure 9 are 6.0 and 8.3 μ A/cm² (electrode surface area = 0.03 cm^2), respectively, which are greater than the newly reported values of 1.2-1.5 μ A/cm² by 5-7 times.³⁷ This indicates that the one-step, biocatalytically generated composite could provide large loading and good activity of the enzyme for the catalytic reaction. There was a slight difference of the maximum reaction rates between Ppy/LOD and Ppy/CNT/LOD. This might be due to the different formation mechanisms of the nanocomposites. The competition between CNT and LOD during the polymerization of the 3-component nanocomposite could make less LOD loading in the sensing layer. However, Ppy/CNT/LOD showed much higher conductivity than Ppy/ LOD as shown in Figure 10. It has been reported that CNTcontaining Ppy has dramatically different conductivity compared to Ppy without CNT doping. 17,23 Figure 10 displays the current voltage (I-V) traces of Ppy-LOD and Ppy-CNT-LOD nanocomposites. Both profiles of Ppy-LOD and Ppy-CNT-LOD composites have the characteristic "S" shapes, reflecting their semiconductor-like characteristics.^{38,39} It appears that trace (a) shows the early linear parts of the increases, which makes it a more ohmic-like property. That means that the electron flow within the composite is enhanced, that is, better conductivity by addition of CNTs in the Ppy-LOD composite, ²³ and indicates that the nanocomposite could be directly used for electron transfer for electronic devices.

Conclusion

A method for biocatalytic generation of Ppy-LOD and Ppy-LOD-CNT nanocomposites was investigated in this work. Lactate oxidase was used to initiate the polymerization of pyrrole monomer in presence of lactate. In terms of the results, different mechanisms for the formation of Ppy-LOD and Ppy-LOD-CNT nanocomposites are proposed. (1) Without CNTs, enzyme molecules served as the seeds for polymerization accompanied with self-assembly of the Ppy-LOD nanoparticles and further formation of "necklace", "network", and even "film" nanostructured composites. (2) With addition of CNTs into the reaction system, the Ppy formation mechanism was changed. The CNTs functioned as the seeds for Ppy formation instead. The nanoparticles-based network formed in mechanism 1 changed to a CNT-networked composite nanofilm. FE-SEM and TEM images showed that the morphology and the thickness of the composite films could be controlled by reaction time and the ratio of pyrrole:CNTs:enzyme. The tailorability, controllability, and the mechanism of the Ppy-LOD-CNT formation showed in this work could provide a universal approach to synthesize nanostructured composites with different nanomaterials and biomolecules for different nanoelectronics and biomedical devices. The application of the nanocomposite for the lactase biosensor and the effects of components of the nanocomposite on both sensing and electronic properties were also studied, demonstrating their novelty and superior properties.

Acknowledgment. This work was financially supported by Singapore DSO (Defence Science Organization) under grant contract DSOCL04135 and by Center for Advanced Bionanosystems, Nanyang Technological University.

References and Notes

- (1) Gerard, M.; Chaubey, A.; Malhotra, B. D. Biosens. Bioelectron. 2002, 17, 345.
- (2) Malinauskas, A.; Garjonyte, R.; Mazeikiene, R.; Jureviciute, I. Talanta 2004, 64, 121.
- (3) Geetha, S.; Rao, C. R. K.; Vijayan, M.; Trivedi, D. C. Anal. Chim. Acta 2006, 568, 119.
- (4) Szunerits, S.; Bouffier, L.; Calemczuk, R.; Corso, B.; Demeunynck, M.; Descamps, E.; Defontaine, Y.; Fiche, J. B.; Fortin, E.; Livache, T.; Mailley, P.; Roget, A.; Vieil, E. *Electroanalysis* **2005**, *17*, 2001.
- (5) Li, C. M.; Chen, W.; Yang, X.; Sun, C. Q.; Gao, C.; Zheng, Z. X.; Sawyer, J. Front. Biosci. 2005, 10, 2518.

- (6) Li, C. M.; Pan, L. K.; Luong, J. H. T. Analyst 2006, 131, 788.
- (7) Li, C. M.; Sun, C. Q.; Chen, W.; Pan, L. Surf. Coat. Technol. 2005, 198, 474.
- (8) Ionescu, R. E.; Gondran, C.; Gheber, L. A.; Cosnier, S.; Marks, R. S. Anal. Chem. **2004**, *76*, 6808.
- (9) Dong, H.; Li, C. M.; Chen, W.; Zhou, Q.; Zeng, Z. X.; Luong, J. H. T. Anal. Chem. 2006, 78, 7424.
- (10) Li, C. M.; Sun, C. Q.; Song, S.; Choong, V. E.; Maracas, G.; Zhang, X. J. Front. Biosci. **2005**, 10, 180.
- (11) Riccardi, C. D.; Yamanaka, H.; Josowicz, M.; Kowalik, J.; Mizaikoff, B.; Kranz, C. Anal. Chem. 2006, 78, 1139.
- (12) Ionescu, R. E.; Abu-Rabeah, K.; Cosnier, S.; Durrieu, C.; Chovelon, J. M.; Marks, R. S. *Electroanalysis* **2006**, *18*, 1041.
- (13) Wang, Z. X.; Roberge, C.; Wan, Y.; Dao, L. H.; Guidoin, R.; Zhang, Z. J. Biomed. Mater. Res., Part A 2003, 66A, 738.
 - (14) Iijima, S. Nature 1991, 354, 56.
- (15) Thostenson, E. T.; Ren, Z. F.; Chou, T. W. Compos. Sci. Technol. 2001, 61, 1899.
- (16) Wildgoose, G. G.; Banks, C. E.; Compton, R. G. Small 2006, 2, 182
- (17) Chen, G. Z.; Shaffer, M. S. P.; Coleby, D.; Dixon, G.; Zhou, W. Z.; Fray, D. J.; Windle, A. H. *Adv. Mater.* **2000**, *12*, 522.
- (18) Zhang, X. T.; Zhang, J.; Wang, R. M.; Zhu, T.; Liu, Z. F. *ChemPhysChem* **2004**, *5*, 998.
 - (19) Zhang, X. T.; Zhang, J.; Liu, Z. F. Carbon 2005, 43, 2186.
- (20) Frackowiak, E.; Khomenko, V.; Jurewicz, K.; Lota, K.; Beguin, F. J. Power Sources 2006, 153, 413.
- (21) Callegari, A.; Cosnier, S.; Marcaccio, M.; Paolucci, D.; Paolucci, F.; Georgakilas, V.; Tagmatarchis, N.; Vazquez, E.; Prato, M. *J. Mater. Chem.* **2004**, *14*, 807.
 - (22) Cosnier, S. Electroanalysis 2005, 17, 1701.
 - (23) Wang, J.; Dai, J. H.; Yarlagadda, T. Langmuir 2005, 21, 9.
- (24) Ramanavicius, A.; Kausaite, A.; Ramanaviciene, A.; Acaite, J.; Malinauskas, A. *Synth. Met.* **2006**, *156*, 409.
- (25) Henry, M. C.; Hsueh, C. C.; Timko, B. P.; Freund, M. S. J. Electrochem. Soc. 2001, 148, D155.
 - (26) Baron, R.; Zayats, M.; Willner, I. Anal. Chem. 2005, 77, 1566.
- (27) Riskin, M.; Basnar, B.; Chegel, V. I.; Katz, E.; Willner, I.; Shi, F.; Zhang, X. J. Am. Chem. Soc. **2006**, 128, 1253.
- (28) Basnar, B.; Weizmann, Y.; Cheglakov, Z.; Willner, I. *Adv. Mater.* **2006**, *18*, 713.
- (29) Riemenschneider, L.; Blank, S.; Radmacher, M. Nano Lett. 2005, 5, 1643.
- (30) Ramanavicius, A.; Kausaite, A.; Ramanaviciene, A. Sens. Actuators, B 2005, 111, 532.
- (31) Chen, Q.; Kenausis, G. L.; Heller, A. J. Am. Chem. Soc. 1998, 120, 4582.
- (32) Bredas, J. L.; Scott, J. C.; Yakushi, K.; Street, G. B. *Phys. Rev. B* **1984**, *30*, 1023.
- (33) Aguilar-Hernandez, J.; Potje-Kamloth, K. Phys. Chem. Chem. Phys. 1999, 1, 1735.
- (34) Kim, D. Y.; Lee, J. Y.; Moon, D. K.; Kim, C. Y. Synth. Met. 1995,
- (35) Bufon, C. C. B.; Vollmer, J.; Heinzel, T.; Espindola, P.; John, H.;
- Heinze, J. J. Phys. Chem. B 2005, 109, 19191. (36) Zhang, X. Y.; Goux, W. J.; Manohar, S. K. J. Am. Chem. Soc.
- (36) Zhang, X. Y.; Goux, W. J.; Manohar, S. K. J. Am. Chem. Soc. **2004**, *126*, 4502.
- (37) Parra, A.; Casero, E.; Vazquez, L.; Pariente, F.; Lorenzo, E. *Anal. Chim. Acta* **2006**, *555*, 308.
 - (38) Lee, H. J.; Park, S. M. J. Phys. Chem. B 2004, 108, 1590.
- (39) Saha, S. K.; Su, Y. K.; Lin, C. L.; Jaw, D. W. Nanotechnology **2004**, *15*, 66.